DMD Fast Forward. Published on January 7, 2014 as doi:10.1124/dmd.113.055590
This article has not been copyedited and formatted. The final version may differ from this version.

DMD #55590

Use of Cassette Dosing Approach to Examine the Effects of P-glycoprotein on the Brain and Cerebral Spinal Fluid Concentrations in Wild-Type and P-glycoprotein Knockout Rats

Xingrong Liu, Jonathan Cheong, Xiao Ding, and Gauri Deshmukh

Genentech Inc., South San Francisco, California (XL, JC, XD, and GD)

Running title: Brain Penetration in Wild-Type and P-gp Knockout Rats

*Address correspondence to:

Xingrong Liu, Ph.D.

Genentech, Inc.

1 DNA Way

South San Francisco, CA 94080

TEL: (650) 467-3505

FAX: (650) 467-3487

E-mail: liu.xingrong@gene.com

The number of text pages: 24

The number of tables: 3

The number of figures: 7

The number of references: 38

The number of words in abstract: 250

The number of words in introduction: 675

The number of words in discussion: 1489

Abbreviations: AUC, area under the concentration-time curve; BBB, blood-brain barrier; BCSFB, blood-CSF barrier; BCRP, human breast cancer resistance protein; Bcrp, rodent breast cancer resistance protein; $C_{u,brain}$, unbound brain concentration; $C_{u,CSF}$, unbound CSF concentration; $C_{u,plasma}$, unbound plasma concentration; $C_{u,brain}/C_{u,CSF}$, unbound brain to CSF concentration ratio; CSF, cerebral spinal fluid; $f_{u,brain,}$ unbound drug fraction in brain, $f_{u,brain,}$ unbound drug fraction in plasma; K_p, brain-to-plasma concentration ratio; $K_{p,uu,brain}$, unbound brain-to-plasma concentration ratio; $K_{p,uu,CSF}$, unbound CSF-to-plasma ratio; LLOQ, lower limit of quantitation; P-gp, P-glycoprotein.

DMD Fast Forward. Published on January 7, 2014 as DOI: 10.1124/dmd.113.055590
This article has not been copyedited and formatted. The final version may differ from this version.

Abstract

The study objectives were to (1) test the hypothesis that the lack of P-glycoprotein (P-gp) and breast cancer resistance protein (Bcrp) inhibition at the blood-brain barrier following cassette dosing of potent P-gp and Bcrp inhibitors was due to low plasma concentrations of those inhibitors and (2) examine the effects of P-gp on the unbound brain ($C_{u,brain}$) and cerebral spinal fluid ($C_{u,CSF}$) concentrations of P-gp substrates in rats. In vitro inhibition of 11 compounds (amprenavir, citalopram, digoxin, elacridar, imatinib, Ko143, loperamide, prazosin, quinidine, sulfasalazine and verapamil) on P-gp and Bcrp was examined in P-gp-expressing and Bcrp-expressing MDCK cells, respectively. An in vivo study was conducted in wild-type and Mdr1a(-/-) rats following subcutaneous cassette dosing of the 11 compounds at 1-3 mg/kg and the brain, CSF and plasma concentrations of these compounds were determined. At the maximal unbound concentrations observed in rats at 1-3 mg/kg, P-gp and Bcrp were not inhibited by a cassette of the 11 compounds. For non-P-gp/Bcrp substrates, similar $C_{u,brain}$, $C_{u,CSF}$, and unbound plasma concentrations ($C_{u,plasma}$) were observed in wild-type and P-gp knockout rats. For P-gp/Bcrp substrates, $C_{u,brain} \leq C_{u,CSF} \leq C_{u,plasma}$ in wild-type rats but $C_{u,brain}$ and $C_{u,CSF}$ increased in the P-gp knockout rats and were within 3-fold of $C_{u,plasma}$ for 6 of the 7 P-gp substrates. These results indicate that P-gp and Bcrp inhibition at the blood-brain barrier is unlikely in cassette and also suggest that P-gp and Bcrp activity at the blood-CSF barrier is functionally not important in determination of the CSF concentration for their substrates.

DMD Fast Forward. Published on January 7, 2014 as DOI: 10.1124/dmd.113.055590
This article has not been copyedited and formatted. The final version may differ from this version.

Introduction

The brain is protected by the blood-brain barrier (BBB), which is formed by the cerebral endothelia, and the blood cerebral spinal fluid barrier (BCSFB), which is formed by the choroid plexus epithelia (Davson and Segal, 1995). The main mechanisms that limit the delivery of drugs from blood into the brain are very low paracellular permeability of the BBB and the multiple drug transporters expressed at the BBB. Two efflux drug transporters, P-glycoprotein (P-gp/MDR1/ABCB1) and breast cancer resistance protein (BCRP/ABCG2), are the main efflux transporters expressed at the luminal side of the BBB, and their functional importance in limiting brain penetration of their substrates has been extensively demonstrated (Agarwal et al., 2011; Breedveld et al., 2005; Chen et al., 2003; Enokizono et al., 2007; Gazzin et al., 2008; Kodaira et al., 2010; Polli et al., 2009; Schinkel et al., 1994; Zhou et al., 2009). At the BCSFB, P-gp and BCRP are expressed at the apical membrane, and the orientation of these transporters indicates influx of their substrates into the CSF (Rao et al., 1999; Zhuang et al., 2006).

A useful parameter to assess the efficiency of a drug crossing the BBB is the ratio of unbound brain concentration to unbound plasma concentration ($K_{p,uu,brain}$) (Hammarlund-Udenaes et al., 2009; Liu et al., 2008). The common method of estimating $K_{p,uu,brain}$ is to determine the in vivo plasma and brain concentration ratio (K_p) and the in vitro unbound fraction in plasma and brain tissue (Kalvass and Maurer, 2002). In order to increase the throughput and reduce resource consumption in determination of K_p, we demonstrated in a previous study that cassette dosing (dosing a mixture of compounds) generated similar K_p values to discrete dosing (dosing an individual compound) for 11 compounds, namely amprenavir, citalopram, digoxin, elacridar, imatinib, Ko143, loperamide, prazosin, quinidine, sulfasalazine, and verapamil in mice (Liu et al., 2012). The 11 compounds in this study can be classified into four groups according to our previous results (Liu et al., 2012): 1) non-P-gp substrate: citalopram, 2) P-gp substrates: amprenavir, digoxin, loperamide, quinidine, verapamil, 3) Bcrp substrates: sulfasalazine, and 4) P-gp/Bcrp dual substrates elacridar, imatinib, prazosin. Quinidine, Ko143, and elacridar are considered to be a P-gp inhibitor, Bcrp inhibitor, and P-gp/Bcrp dual inhibitor, respectively. These 11 compounds were selected to create the “worst case” scenario of potential drug-drug

interactions at the BBB as this group of compounds contains known potent P-gp and Bcrp inhibitors and typical P-gp and Bcrp substrates. However, no drug-drug interactions at the BBB were observed in our previous study in mice when these 11 compounds were dosed in a cassette at 1-3 mg/kg (Liu et al., 2012). We hypothesized that plasma concentrations generated following a cassette dosing at 1-3 mg/kg for each compound were too low to cause any significant drug-drug interactions at the BBB. To test this hypothesis, we examined the brain penetration in rats for the same 11 compounds dosed as a cassette and discretely and assessed the in vitro inhibition of P-gp and Bcrp in P-gp- or Bcrp-expressing cells.

The CSF is in direct contact with brain tissue, and, therefore, the CSF is assumed to readily equilibrate with brain interstitial fluid (Meineke et al., 2002; Shen et al., 2004). CSF drug concentrations have been used as a common surrogate for unbound brain concentrations in clinical studies (Bonati et al., 1982; Cherubin et al., 1989; Garver, 1989; Ostermann et al., 2004; Reiter and Doron, 1996). Nevertheless, the reliability of using CSF drug concentration as a substitute has been challenged as the transport direction is different between the BBB and BCSFB for the two main efflux drug transporters, P-gp and BCRP (Bonati et al., 1982; de Lange, 2013; de Lange and Danhof, 2002; Kalvass et al., 2013; Kusuhara and Sugiyama, 2004; Rao et al., 1999; Zhuang et al., 2006). Furthermore, Gazzin et al. (2008) reported that choroid plexus-associated P-gp content was less than 0.5% of the level in the cerebral microvessels, indicating P-gp efflux is not important at the BCSFB. However, the functional importance of P-gp and Bcrp in governing the CSF concentration of their substrates has not been extensively examined. In order to examine the effects of P-gp and Bcrp efflux on the brain and CSF drug concentrations, we investigated the CSF, plasma and unbound brain concentrations for the 11 compounds in P-gp competent and P-gp deficient rats.

Materials and Methods

Chemicals. Citalopram, digoxin, loperamide, prazosin, quinidine, sulfasalazine, and verapamil were obtained from Sigma-Aldrich (St. Louis, MO). Amprenavir, amprenavir-D4, elacridar, and imatinib were obtained from Toronto Research Chemicals, Inc. (North York, ON, Canada). Ko143 was from Enzo Life Sciences Inc. (Farmingdale, NY). All chemicals used in the experiments were of the highest available grade.

Plasma protein binding. The unbound fractions in plasma and brain homogenate for the 11 compounds were determined in a 48-well rapid equilibrium dialysis (RED) device using a dialysis membrane with a molecular weight cut-off value of 8000 Da (Pierce Biotechnology, Rockford, IL). Blank plasma was spiked with the 11 compounds at a final concentration of 5 µM. A total of 300 µL of plasma with compound was added to the donor side and 500 µL of buffer was added to the receiver side. The plate was placed on a rocking platform at 400 rpm with 1 mm radius agitation for 4 hr at 37ºC. A volume of 20 µL each of buffer and plasma samples were transferred to a 96-well plate, and 20 µL of blank plasma and buffer were added to the buffer and plasma samples, respectively. Plasma proteins were precipitated using 65% acetonitrile containing internal standard (0.1 µM propranolol). Drug concentrations were quantitated by liquid chromatography-tandem mass spectrometry (LC-MS/MS), and the unbound fraction in plasma ($f_{u,p}$) and unbound fraction in the brain homogenate ($f_{u,homogenate}$) was calculated as the ratio of the buffer concentration versus the plasma concentration.

The unbound fraction in the brain tissue was estimated from the unbound fractions determined in the brain tissue homogenates using Equation 1 (Kalvass and Maurer, 2002).

$$f_{u,b} = \frac{1}{1 + (1/f_{u,\mathrm{hom}ogenate} - 1) \bullet D} \qquad \text{Equation 1}$$

where $f_{u,b}$ represents the unbound fraction in brain tissue and unbound fraction in brain homogenate. D is the dilution factor for the brain homogenate.

In vitro P-gp and Bcrp transport assay. MDCK cells transfected with the human MDR1 gene (MDR1-MDCK) or transfected with the mouse Bcrp gene (Bcrp1-MDCK) were maintained at 37°C, 95% humidity, and 5% CO2 in culture with Eagle's minimum essential medium (0.1%

DMD Fast Forward. Published on January 7, 2014 as DOI: 10.1124/dmd.113.055590
This article has not been copyedited and formatted. The final version may differ from this version.

nonessential amino acids, 1 mM sodium pyruvate, 2 mM L-glutamine, 1.5 g/L sodium bicarbonate) supplemented with 10% fetal bovine serum. The MDCKI–MDR1 cell medium was further supplemented with 0.2 µM colchicine to sustain MDR1 expression. The monolayers were equilibrated for 30 min in transport buffer (Hank's Balanced Salt Solution with 10 mM HEPES, pH 7.4) at 37°C with 5% CO2 and 95% humidity prior to the experiment. Bidirectional transport of amprenavir (1 µM) in MDR1-MDCK cells and prazosin (1 µM) in Bcrp1-MDCK cells was assessed in the presence and absence of the other ten compounds individually or as a mixture of them at approximately the in vivo maximal total and unbound concentrations in rats. The concentrations of amprenavir and prazosin were determined by LC-MS/MS and their apparent permeability (P_{app}) from the apical-to-basolateral (A to B) and basolateral-to-apical (B to A) directions was calculated using Equation 2:

$$P_{app} = \frac{dQ}{dt} \bullet \frac{1}{C_0} \bullet \frac{1}{A} \qquad \text{Equation 2}$$

where dQ/dt is the rate of compound appearance in the receiver compartment, C_0 is the concentration in the donor compartment at time = 0, and A is the surface area of the insert.

Animal experiments. Male Sprague-Dawley (wild type, WT) and Mdr1a(-/-) rats (P-gp knockout, KO) weighing 250-350 g were obtained from Sigma Advanced Genetic Engineering Labs (SAGE, Boyertown, PA). Upon arrival, the rats were maintained for at least 5 days on a 12-h light/dark cycle in a temperature- and humidity-controlled environment with free access to food and water. Two in vivo studies were conducted in the present study. In Study #1, the 11 compounds were dosed discretely or as a cassette in the WT rats to examine the consistency between discrete and cassette dosing. In Study #2, the 11 compounds were dosed as a cassette in WT and P-gp KO mice to investigate the effects of P-gp transport on brain and CSF drug concentrations. In the discrete dosing study, rats were administered a single subcutaneous dose (n = 3 per time point) of a single compound or a cassette of the 11 compounds at 1 mg/kg for citalopram, elacridar, imatinib, loperamide, prazosin, and verapamil and at 3 mg/kg for amprenavir, quinidine, Ko143, digoxin, and sulfasalazine. Subcutaneous administration was selected as this route allows for dosing either a solution or a suspension in the drug discovery

DMD Fast Forward. Published on January 7, 2014 as DOI: 10.1124/dmd.113.055590
This article has not been copyedited and formatted. The final version may differ from this version.

setting. Each compound was completely dissolved in 100% N-methyl-2-pyrrolidone and dosed at 1 mL/kg. Rats were euthanized in a CO_2 chamber at 0.25, 1, and 3 hr post dose. Whole blood was collected by cardiac puncture into Microtainer tubes (BD Biosciences, San Jose, CA) containing heparin and stored on ice until centrifuged for the preparation of plasma. Approximately 50 µL of each CSF sample was collected via cisterna magna puncture, mixed with 100 µL blank plasma to avoid nonspecific binding, and stored at -20°C before analysis. Whole brains were collected by decapitation, rinsed in phosphate-buffered saline, weighed, and immediately frozen on dry ice. All studies were conducted in accordance with approved Genentech Animal Care and Use Procedures.

Sample analysis. Standard curves and quality control samples were prepared by spiking a known amount of a mixture of the 11 compounds into a blank mixed matrix of rat plasma, brain homogenate, and CSF (1:1:1, v/v/v). The brain tissue of each rat was homogenized in four volumes (w/v) of water. A volume of 25 µL of each plasma sample was mixed with 25 µL of blank brain homogenate and 25 µL of blank CSF. Likewise, 25 µL of each brain homogenate sample was mixed with 25 µL of blank plasma and 25 µL of blank CSF, and 25 µL of each CSF sample was mixed with 25 µL of blank plasma and 25 µL of blank brain homogenate. The resulting 75 µL of samples, 75 µL of calibration standards, or 75 µL of quality controls were mixed with 15 µL of internal standard (amprenavir-D4) and 225 µL acetonitrile. Following vortexing and centrifugation at 1500 x g for 10-15 minutes, 160 µL of supernatant was transferred to a 96-well plate and diluted with 40 µL water prior to analysis by high performance LC-MS/MS.

Samples were analyzed using two sets of standard curves and two sets of quality controls in each analytical run. The system consisted of an Accela pump (Thermo Scientific, Waltham, MA), an HTS-PAL autosampler (Leap Technologies, Switzerland), and an AB Sciex API 5000 (AB Sciex, Foster City, CA) mass spectrometer with a turbo ion spray interface. A 20 µL aliquot of each sample was injected onto a reverse-phase HALO C18 column. The lower limit of quantitation (LLOQ) for the compounds in the mixed matrix ranged from 0.122 to 3.91 ng/mL. The assay accuracy was between 75% and 125%.

DMD Fast Forward. Published on January 7, 2014 as DOI: 10.1124/dmd.113.055590
This article has not been copyedited and formatted. The final version may differ from this version.

Data analysis. The total brain drug concentration was corrected for the residual blood in the brain vasculature by subtracting 1.03% of the plasma concentration determined in the corresponding samples (Friden et al., 2010). The area under the concentration-time curve (AUC) values were calculated using the trapezoid rule from 0 to 3.0 hr. The brain-to-plasma concentration ratio (K_p), unbound brain-to-plasma concentration ratio ($K_{p,uu,brain}$), unbound CSF-to-plasma concentration ratio ($K_{p,uu,CSF}$), and unbound brain-to-CSF ratio ($C_{u,brain}/C_{u,CSF}$) were calculated using Equations 3-6:

$$K_p = \frac{AUC_b}{AUC_p} \qquad \text{Equation 3}$$

$$K_{p,uu,Brain} = \frac{AUC_b}{AUC_p} \bullet \frac{f_{u,b}}{f_{u,p}} \qquad \text{Equation 4}$$

$$K_{p,uu,CSF} = \frac{AUC_{CSF}}{AUC_p} \bullet \frac{f_{u,CSF}}{f_{u,p}} \qquad \text{Equation 5}$$

$$C_{u,brain} / C_{u,CSF} = \frac{AUC_b \bullet f_{u,b}}{AUC_{CSF} \bullet f_{u,CSF}} \qquad \text{Equation 6}$$

where AUC_b, AUC_p, and AUC_{CSF} represent the AUC values of plasma, brain, and CSF from 0 to 3 hr, respectively, and $f_{u,CSF}$ represents the unbound fraction in the CSF, which was calculated from $f_{u,p}$ according to the method reported by Friden et al. (2009).

The variances of the AUCs and their ratios were calculated using the first order Taylor series expansion of the AUCs and their ratios. The KO/WT ratios were compared using log-transformed ratios were done using two-tailed t-test with equal variances.

Results

In vitro assessment of P-gp and Bcrp inhibition. The unbound drug fractions in plasma and brain tissue of the 11 compounds are shown in Table 1. The effects of the 11 compounds dosed discretely or as a cassette on the transport of amprenavir, a model P-gp substrate, in human P-gp-expressing cells (MDR1-MDCK) and on the transport of prazosin, a model Bcrp substrate, in Bcrp-expressing cells are shown in Figure 1 and 2, respectively. At concentrations that are equivalent to the in vivo maximal plasma total concentrations in rats, as presented in the next section, amprenavir efflux was partially inhibited by elacridar, quinidine, Ko143, or a cassette of the 11 compounds such that the $P_{app\ (A\ to\ B)}$ of amprenavir increased from 0.3 x 10^{-6} cm/s to approximately 2 x 10^{-6} cm/s with no appreciable change to the $P_{app\ (B\ to\ A)}$ (Figure 1A). At in vivo maximal unbound concentrations of the 11 compounds, however, no inhibition was observed for either the individual or cassette dosing (Figure 1B). At in vivo maximal total concentrations, prazosin efflux was partially inhibited by elacridar, quinidine, amprenavir, digoxin, sulfasalazine, imatinib, and citalopram such that the $P_{app\ (A\ to\ B)}$ of prazosin increased from 0.2 x 10^{-6} cm/s to 1.3 - 2.3 x 10^{-6} cm/s with no appreciable change to the $P_{app\ (B\ to\ A)}$. Interestingly, prazosin efflux was completely abolished by 800 nM Ko143 or by a cassette of the 11 compounds (Figure 2A). At in vivo maximal unbound concentrations of the 11 compounds, however, no inhibition was observed for either individual or cassette dosing (Figure 2B). Since the in vivo plasma concentration of Ko143 was below the LLOQ, 800 nM Ko143 was selected to examine the Bcrp inhibition at a high Ko143 concentration. A concentration of 0.02 nM Ko143 was selected as its unbound plasma concentration based on its plasma LLOQ (1 nM) and its plasma protein binding. These in vitro results demonstrate that the efflux of P-gp and Bcrp cannot be inhibited by the 11 compounds individually or as a cassette at their in vivo observed maximal unbound concentrations.

Comparison of plasma, brain and CSF concentrations between discrete and cassette dosing in WT rats in Study #1. The plasma, brain and CSF concentration-time profiles for 10 of the 11 compounds following a single subcutaneous administration at 1 or 3 mg/kg in either discrete or cassette dosing in WT rats are shown in Figure 3. Ko143 plasma, brain and

DMD Fast Forward. Published on January 7, 2014 as DOI: 10.1124/dmd.113.055590
This article has not been copyedited and formatted. The final version may differ from this version.

CSF concentrations were below the LLOQ at all the time points. The brain concentration of sulfasalazine and CSF concentrations of sulfasalazine and elacridar were all below the LLOQ. In general, similar plasma, brain and CSF concentration-time profiles were observed for discrete and cassette dosing. The AUC values for plasma, brain, and CSF and the $K_{p,uu,brain}$, $K_{p,uu,CSF}$, and $C_{u,brain}/C_{u,CSF}$ from discrete and cassette dosing are listed in Table 2. A good correlation was observed for the $K_{p,uu,brain}$ and $K_{p,uu,CSF}$ from the discrete and cassette dosing with $R^2 = 0.94$ for the $K_{p,uu,brain}$ and $R^2 = 0.66$ for the $K_{p,uu,CSF}$ (Figure 4). The low R^2 for $K_{p,uu,CSF}$ perhaps is due to low CSF concentration and fewer data points. All the ratios were within 3-fold between the discrete and cassette dosing. These results demonstrate that brain, CSF and plasma concentrations are similar following cassette and discrete administration in rats.

Plasma, brain and CSF concentrations following cassette dosing in WT or P-gp KO rats in Study #2. The plasma, brain and CSF concentration-time profiles for 10 of the 11 compounds following cassette dosing in WT and P-gp KO rats are shown in Figure 5. The Ko143 concentration was below the LLOQ for all time points. The brain concentration of sulfasalazine and CSF concentrations of sulfasalazine and elacridar were all below the LLOQ. Similar plasma concentrations were observed between the WT and KO rats, but the brain and CSF concentrations were generally higher in the KO rats.

The AUC values for plasma, brain, CSF, $K_{p,uu,brain}$, $K_{p,uu,CSF}$, and $C_{u,brain}/C_{u,CSF}$ in WT and P-gp KO rats are listed in Table 3 and presented in Figure 6. For the non-P-gp substrate, citalopram, $K_{p,uu,brain}$ was near unity in the WT and KO rats (Figure 6A). The $K_{p,uu,brain}$ values for the five P-gp substrates, amprenavir, loperamide, digoxin, verapamil, and quinidine, were lower than unity, ranging from 0.013 to 0.18 in the WT rats and ranging from 0.18 to 3.4 in KO rats, an increase of 14- to 54-fold. For the P-gp/Bcrp dual substrates, elacridar, imatinib and prazosin, the $K_{p,uu,brain}$ values were lower than unity, ranging from 0.092 to 0.39 in WT rats and ranging from 0.17 to 1.9 in KO rats, an increase of 2- to 5-fold. To compare the effects of P-gp in rats and mice, we present the ratio of K_p in P-gp KO rats versus that in WT rats (KO/WT) and the KO/WT in P-gp KO the mice versus WT mice (Figure 7). The rat KO/WT ratios were calculated from the data in Table 3, and the mouse KO/WT ratios were derived from previously reported results (Liu et al.,

DMD Fast Forward. Published on January 7, 2014 as DOI: 10.1124/dmd.113.055590
This article has not been copyedited and formatted. The final version may differ from this version.

2012). A good agreement was observed for the KO/WT ratios of K_p in rats and mice, with R^2 = 0.91, and KO/WT ratios within 3-fold between these two species. Interestingly, a regression analysis resulted in KO/WT(mouse) = 0.495[(KO/WT(rat)]$^{1.04}$, indicating that mouse P-gp at the BBB has similar or a slightly lower efflux activity than rat P-gp.

The effects of P-gp mediated efflux on the $C_{u,brain}/C_{u,CSF}$ ratio and $K_{p,uu,CSF}$ are presented in Figures 6B and 6C. For the non-P-gp substrate, citalopram, the $C_{u,brain}/C_{u,CSF}$ and $K_{p,uu,CSF}$ were near unity in both WT and KO rats; therefore, $C_{u,brain} \approx C_{u,CSF} \approx C_{u,plasma}$. The $C_{u,brain}/C_{u,CSF}$ and $K_{p,uu,CSF}$ values were below unity for the P-gp substrates (amprenavir, loperamide, digoxin, verapamil, and quinidine) and P-gp/Bcrp dual substrates (elacridar, imatinib and prazosin) in WT rats; therefore, $C_{u,brain} < C_{u,CSF} < C_{u,plasma}$ for these compounds. If considering 3-fold as the limit of experimental uncertainty, then $C_{u,brain} \leq C_{u,CSF} \leq C_{u,plasma}$ in WT rats. In P-gp KO rats, both $C_{u,brain}/C_{u,CSF}$ and $K_{p,uu,CSF}$ increased for the P-gp substrates and the P-gp/Bcrp dual substrates compared to P-gp competent rats, and the $C_{u,brain}$, $C_{u,CSF}$, and C_{up} were within 3-fold for all compounds except loperamide, whose $C_{u,brain}$ and $C_{u,CSF}$ were approximately 4-fold.

DMD Fast Forward. Published on January 7, 2014 as DOI: 10.1124/dmd.113.055590
This article has not been copyedited and formatted. The final version may differ from this version.

Discussion

The present study was designed to test the hypothesis that the lack of P-gp or Bcrp inhibition at the BBB in our previous study in mice following cassette dosing of P-gp or Bcrp substrates and inhibitors was due to low plasma concentrations of those inhibitors (Liu et al., 2012). This hypothesis is supported by the observation in the present study that at the concentrations corresponding to in vivo unbound concentrations for the 11 compounds, no P-gp or Bcrp inhibition was observed in the P-gp- or Bcrp-expressing cell lines, respectively. The present study was also designed to examine the effects of P-gp on the unbound brain and CSF concentrations of P-gp substrates. Our study shows that for a non-P-gp/Bcrp substrate, $C_{u,brain}$, $C_{u,CSF}$, and $C_{u,plasma}$ were similar in WT and P-gp KO rats. For P-gp/Bcrp dual substrates, $C_{u,brain} \leq C_{u,CSF} \leq C_{u,plasma}$ in WT rats, but in P-gp KO mice the $C_{u,brain}$ and $C_{u,CSF}$ increased and the difference between these concentrations reduced to less than 3-fold for 6 of 7 compounds compared to P-gp competent rats.

Our previous study showed that P-gp and Bcrp at the BBB was not inhibited when 11 compounds, including typical P-gp and Bcrp substrates and potent P-gp and Bcrp inhibitors, were administrated subcutaneously at 1-3 mg/kg in mice (Liu et al., 2012). To confirm this observation, we examined the plasma and brain concentrations following discrete and cassette dosing of the same 11 compounds in rats in the present study. The $C_{u,brain}$ and $C_{u,CSF}$ values were similar between the discrete and cassette dosing, indicating a lack of drug-drug interactions due to P-gp or Bcrp inhibition at the BBB following cassette dosing in rats. Furthermore, in the present study, the KO/WT ratios of K_p in rats are within 3-fold of that in mice, indicating that P-gp has similar efflux transport activity at the BBB in rats and mice, which is consistent with the results reported recently by Bundgaard et al. (2012).

We hypothesized that the $C_{u,plasma}$ of the P-gp and/or Bcrp inhibitors were too low to inhibit P-gp and Bcrp at the BBB under our experimental conditions. To test this hypothesis, we assessed in vitro P-gp and Bcrp inhibition of the 11 compounds dosed discretely or as a cassette in P-gp- or Bcrp-expressing cell lines, respectively. These in vitro results demonstrate that the efflux activities of P-gp and Bcrp cannot be inhibited by the 11 compounds at their in vivo

DMD Fast Forward. Published on January 7, 2014 as DOI: 10.1124/dmd.113.055590
This article has not been copyedited and formatted. The final version may differ from this version.

maximal unbound concentrations observed in the in vivo rat cassette dosing study. Unbound concentrations were considered as no plasma was present in the in vitro assay. As expected, at higher concentrations such as at the in vivo maximal total concentrations, partial or full inhibition of P-gp and Bcrp can be observed in the in vitro study.

The in vitro inhibition results are consistent with results reported in the literature for two potent P-gp and/or Bcrp inhibitors: elacridar and Ko143. Elacridar has a K_i of 2.5 nM for P-gp inhibition using digoxin as the P-gp substrate. In the present study, 20 nM of elacridar only partially inhibited P-gp efflux, where amprenavir was used as the P-gp substrate. This discrepancy is likely due to different P-gp substrates being used in these two studies. Elacridar is also a potent Bcrp inhibitor with an in vitro EC_{90} of 51-61 nM (Allen et al., 2002; Sugimoto et al., 2011). Our results are consistent with the reported EC_{90}, as 20 nM elacridar partially inhibited the BCRP substrate prazosin in the present study. Ko143 is a potent and selective BCRP inhibitor with a cell EC_{90} of 23-26 nM (Allen et al., 2002). In the present study, 800 nM Ko143 abolished the BCRP efflux and 0.02 nM only partially inhibited the BCRP efflux. Although Ko143 is a potent inhibitor for BCRP, it cannot be used in vivo in rodents likely due to its high clearance.

The results from the present study indicate that the CSF concentration of P-gp substrates is not determined by P-gp and Bcrp at the BCSFB. It has been demonstrated that drug transporters such as P-gp and Bcrp at the BBB and BCSFB were expressed differently. In the cerebral endothelia, both P-gp and Bcrp are expressed in the luminal side of the plasma membrane; however, in the choroid plexus epithelia, P-gp and Bcrp are expressed in the apical membrane (Rao et al., 1999; Zhuang et al., 2006). The expression of P-gp and Bcrp at the luminal side of the BBB indicates that they efflux their substrates out of the brain. Therefore, the unbound brain concentration is lower than the unbound plasma concentration for P-gp and Bcrp substrates in P-gp and Bcrp competent animals and the unbound brain concentration is similar to the unbound plasma concentration in the P-gp and Bcrp deficient animals, which is supported by extensive data in the literature (Chen et al., 2003; Enokizono et al., 2008; Enokizono et al., 2007; Polli et al., 2009).

DMD Fast Forward. Published on January 7, 2014 as DOI: 10.1124/dmd.113.055590
This article has not been copyedited and formatted. The final version may differ from this version.

The expression of P-gp and Bcrp at the apical side of the BCSFB predicts that these transporters influx their substrates from blood into the CSF. Therefore, if P-gp and Bcrp are functionally important, the CSF concentration of P-gp and Bcrp substrates should be higher than their unbound plasma concentration in P-gp competent animals, and their CSF concentration is expected to decrease in the P-gp deficient animals. However, this is inconsistent with observations from the present study in rats. We observed that the CSF concentration of P-gp/Bcrp substrates was lower than the unbound plasma concentration in the P-gp competent rats, and their CSF concentration increased in the P-gp deficient rats. Previous results from P-gp competent and P-gp or P-gp/Bcrp deficient mice also do not support this prediction. In a large study of 34 CNS drugs and eight P-gp substrates in WT and P-gp KO mice, the CSF concentration was essentially lower than the unbound plasma concentration for all the compounds in WT mice, and the CSF concentration either did not change or increased in the P-gp KO mice (Doran et al., 2005; Maurer et al., 2005). Kodaira et al. (2011) showed that the CSF concentration of six P-gp or Bcrp substrates was lower than the unbound plasma concentration in WT mice but increased in P-gp/Bcrp KO mice. A study in which the CSF was collected from mouse ventricles also showed similar CSF and unbound plasma concentration for the P-gp/Bcrp substrate topotecan (Zhuang et al., 2006). Therefore, the observed experimental results indicate that P-gp and Bcrp efflux at the BCSFB is functionally not important. This conclusion is consistent with the low expression of P-gp at the choroid plexus (Gazzin et al., 2008). The underlying mechanism leading to the CSF concentration being between the unbound brain and unbound plasma concentrations for P-gp and Bcrp substrates is perhaps a result of a partial exchange between CSF and brain tissue at the ependyma on the ventricle surface, as there is no barrier between the two at this location. In addition, part of the CSF originates from the brain interstitial fluid.

Our data from the present study shows that for one non-P-gp/Bcrp substrate, $C_{u,brain} \approx C_{u,CSF} \approx C_{up}$, and for seven P-gp/Bcrp substrates, $C_{u,brain} \leq C_{u,CSF} \leq C_{u,plasma}$, in WT rats. This observation was consistent with previously reported results (Friden et al., 2009; Kodaira et al., 2011; Liu et al., 2006; Liu et al., 2009). We previously showed that for five non-efflux substrates,

DMD Fast Forward. Published on January 7, 2014 as DOI: 10.1124/dmd.113.055590
This article has not been copyedited and formatted. The final version may differ from this version.

$C_{u,brain} \approx C_{u,CSF} \approx C_{up}$, and for one P-gp substrate, $C_{u,brain} \approx C_{u,CSF} < C_{u,plasma}$ in rats (Liu et al., 2006). Friden et al. (2009) observed that $C_{u,brain}$ was within 3-fold of the $C_{u,CSF}$ for 33 of 39 compounds, while $C_{u,brain} < C_{u,CSF}$ for the six P-gp substrates. Similarly, Kodaira et al. (2011) observed that the $C_{u,brain}$ values were within 3-fold of the $C_{u,CSF}$ for 18 of 25 compounds, and $C_{u,brain} < C_{u,CSF}$ for seven P-gp or Bcrp substrates. Therefore, for non-efflux substrates, the CSF concentration can be used to predict the unbound brain concentration, but for P-gp/Bcrp substrates, CSF concentration may overpredict the unbound brain concentration and CSF concentration represents the maximal unbound brain concentration.

In summary, the present study demonstrates that inhibition of P-gp at the BBB is unlikely in cassette dosing for the compounds dosed at 1-3 mg/kg, supporting the use of a cassette dosing approach to study brain penetration. Our work in P-gp competent and deficient rats further supports the notion that unbound brain, CSF and plasma drug concentrations were similar for non-efflux substrates. Furthermore, the unbound brain concentration is generally less than the CSF concentration, and the CSF concentration is generally less than the unbound plasma concentration for P-gp substrates. The present study is the first to show that the CSF concentration of P-gp/Bcrp substrates was lower than their unbound plasma concentration in P-gp competent rats and their CSF concentration was similar to their unbound plasma concentration in P-gp deficient rats. Our work suggests that P-gp and Bcrp at the BCSFB are perhaps not functionally important in determination of CSF concentration for their substrates.

Acknowledgements

The authors thank Quynh Ho, Jason Halladay, Emile Plise, and Laurent Salphati for their contributions for the in vitro studies and Brian Dean for his support of the bioanalysis.

Authorship Contributions

Participated in research design: Liu, Ding, Cheong, and Deshmukh

Conducted experiments: Ding, Cheong, and Deshmukh

Contributed new reagents or analytical tools: None

Performed data analysis: Deshmukh, Cheong, and Liu

Wrote or contributed to the writing of the manuscript: Liu

References

Agarwal S, Sane R, Ohlfest JR and Elmquist WF (2011) The role of the breast cancer resistance protein (ABCG2) in the distribution of sorafenib to the brain. *J Pharmacol Exp Ther* **336**:223-233.

Allen JD, van Loevezijn A, Lakhai JM, van der Valk M, van Tellingen O, Reid G, Schellens JH, Koomen GJ and Schinkel AH (2002) Potent and specific inhibition of the breast cancer resistance protein multidrug transporter in vitro and in mouse intestine by a novel analogue of fumitremorgin C. *Mol Cancer Ther* **1**:417-425.

Bonati M, Kanto J and Tognoni G (1982) Clinical pharmacokinetics of cerebrospinal fluid. *Clin Pharmacokinet* **7**:312-335.

Breedveld P, Pluim D, Cipriani G, Wielinga P, van Tellingen O, Schinkel AH and Schellens JH (2005) The effect of Bcrp1 (Abcg2) on the in vivo pharmacokinetics and brain penetration of imatinib mesylate (Gleevec): implications for the use of breast cancer resistance protein and P-glycoprotein inhibitors to enable the brain penetration of imatinib in patients. *Cancer Res* **65**:2577-2582.

Bundgaard C, Jensen CJ and Garmer M (2012) Species comparison of in vivo P-glycoprotein-mediated brain efflux using mdr1a-deficient rats and mice. *Drug Metab Dispos* **40**:461-466.

Chen C, Liu X and Smith BJ (2003) Utility of Mdr1-gene deficient mice in assessing the impact of P-glycoprotein on pharmacokinetics and pharmacodynamics in drug discovery and development. *Curr Drug Metab* **4**:272-291.

Cherubin CE, Eng RH, Norrby R, Modai J, Humbert G and Overturf G (1989) Penetration of newer cephalosporins into cerebrospinal fluid. *Rev Infect Dis* **11**:526-548.

Davson H and Segal M (1995) *Physiology of the CSF and blood-brain barriers*, CRC Press, Inc, Boca Raton.

de Lange EC (2013) Utility of CSF in translational neuroscience. *J Pharmacokinet Pharmacodyn* **40**:315-326.

de Lange EC and Danhof M (2002) Considerations in the use of cerebrospinal fluid pharmacokinetics to predict brain target concentrations in the clinical setting: implications of the barriers between blood and brain. *Clin Pharmacokinet* **41**:691-703.

Doran A, Obach RS, Smith BJ, Hosea NA, Becker S, Callegari E, Chen C, Chen X, Choo E, Cianfrogna J, Cox LM, Gibbs JP, Gibbs MA, Hatch H, Hop CE, Kasman IN, Laperle J, Liu J, Liu X, Logman M, Maclin D, Nedza FM, Nelson F, Olson E, Rahematpura S, Raunig D, Rogers S, Schmidt K, Spracklin DK, Szewc M, Troutman M, Tseng E, Tu M, Van Deusen JW, Venkatakrishnan K, Walens G, Wang EQ, Wong D, Yasgar AS and Zhang C (2005) The impact of P-glycoprotein on the disposition of drugs targeted for indications of the central nervous system: evaluation using the MDR1A/1B knockout mouse model. *Drug Metab Dispos* **33**:165-174.

Enokizono J, Kusuhara H, Ose A, Schinkel AH and Sugiyama Y (2008) Quantitative investigation of the role of breast cancer resistance protein (Bcrp/Abcg2) in limiting brain and testis penetration of xenobiotic compounds. *Drug Metab Dispos* **36**:995-1002.

Enokizono J, Kusuhara H and Sugiyama Y (2007) Effect of breast cancer resistance protein (Bcrp/Abcg2) on the disposition of phytoestrogens. *Mol Pharmacol* **72**:967-975.

Friden M, Ljungqvist H, Middleton B, Bredberg U and Hammarlund-Udenaes M (2010) Improved measurement of drug exposure in the brain using drug-specific correction for residual blood. *J Cereb Blood Flow Metab* **30**:150-161.

Friden M, Winiwarter S, Jerndal G, Bengtsson O, Wan H, Bredberg U, Hammarlund-Udenaes M and Antonsson M (2009) Structure-brain exposure relationships in rat and human using a novel data set of unbound drug concentrations in brain interstitial and cerebrospinal fluids. *J Med Chem* **52**:6233-6243.

Garver DL (1989) Neuroleptic drug levels and antipsychotic effects: a difficult correlation; potential advantage of free (or derivative) versus total plasma levels. *J Clin Psychopharmacol* **9**:277-281.

Gazzin S, Strazielle N, Schmitt C, Fevre-Montange M, Ostrow JD, Tiribelli C and Ghersi-Egea JF (2008) Differential expression of the multidrug resistance-related proteins ABCb1 and ABCc1 between blood-brain interfaces. *J Comp Neurol* **510**:497-507.

Hammarlund-Udenaes M, Bredberg U and Friden M (2009) Methodologies to assess brain drug delivery in lead optimization. *Curr Top Med Chem* **9**:148-162.

Kalvass JC and Maurer TS (2002) Influence of nonspecific brain and plasma binding on CNS exposure: implications for rational drug discovery. *Biopharm Drug Dispos* **23**:327-338.

Kalvass JC, Polli JW, Bourdet DL, Feng B, Huang SM, Liu X, Smith QR, Zhang LK and Zamek-Gliszczynski MJ (2013) Why clinical modulation of efflux transport at the human blood-brain barrier is unlikely: the ITC evidence-based position. *Clin Pharmacol Ther* **94**:80-94.

Kodaira H, Kusuhara H, Fujita T, Ushiki J, Fuse E and Sugiyama Y (2011) Quantitative evaluation of the impact of active efflux by p-glycoprotein and breast cancer resistance protein at the blood-brain barrier on the predictability of the unbound concentrations of drugs in the brain using cerebrospinal fluid concentration as a surrogate. *J Pharmacol Exp Ther* **339**:935-944.

Kodaira H, Kusuhara H, Ushiki J, Fuse E and Sugiyama Y (2010) Kinetic analysis of the cooperation of P-glycoprotein (P-gp/Abcb1) and breast cancer resistance protein (Bcrp/Abcg2) in limiting the brain and testis penetration of erlotinib, flavopiridol, and mitoxantrone. *J Pharmacol Exp Ther* **333**:788-796.

Kusuhara H and Sugiyama Y (2004) Efflux transport systems for organic anions and cations at the blood-CSF barrier. *Adv Drug Deliv Rev* **56**:1741-1763.

Liu X, Chen C and Smith BJ (2008) Progress in brain penetration evaluation in drug discovery and development. *J Pharmacol Exp Ther* **325**:349-356.

Liu X, Ding X, Deshmukh G, Liederer BM and Hop CE (2012) Use of the cassette-dosing approach to assess brain penetration in drug discovery. *Drug Metab Dispos* **40**:963-969.

Liu X, Smith BJ, Chen C, Callegari E, Becker SL, Chen X, Cianfrogna J, Doran AC, Doran SD, Gibbs JP, Hosea N, Liu J, Nelson FR, Szewc MA and Van Deusen J (2006) Evaluation of cerebrospinal fluid concentration and plasma free

concentration as a surrogate measurement for brain free concentration. *Drug Metab Dispos* **34**:1443-1447.

Liu X, Van Natta K, Yeo H, Vilenski O, Weller PE, Worboys PD and Monshouwer M (2009) Unbound drug concentration in brain homogenate and cerebral spinal fluid at steady state as a surrogate for unbound concentration in brain interstitial fluid. *Drug Metab Dispos* **37**:787-793.

Maurer TS, Debartolo DB, Tess DA and Scott DO (2005) Relationship between exposure and nonspecific binding of thirty-three central nervous system drugs in mice. *Drug Metab Dispos* **33**:175-181.

Meineke I, Freudenthaler S, Hofmann U, Schaeffeler E, Mikus G, Schwab M, Prange HW, Gleiter CH and Brockmoller J (2002) Pharmacokinetic modelling of morphine, morphine-3-glucuronide and morphine-6-glucuronide in plasma and cerebrospinal fluid of neurosurgical patients after short-term infusion of morphine. *Br J Clin Pharmacol* **54**:592-603.

Ostermann S, Csajka C, Buclin T, Leyvraz S, Lejeune F, Decosterd LA and Stupp R (2004) Plasma and cerebrospinal fluid population pharmacokinetics of temozolomide in malignant glioma patients. *Clin Cancer Res* **10**:3728-3736.

Polli JW, Olson KL, Chism JP, John-Williams LS, Yeager RL, Woodard SM, Otto V, Castellino S and Demby VE (2009) An unexpected synergist role of P-glycoprotein and breast cancer resistance protein on the central nervous system penetration of the tyrosine kinase inhibitor lapatinib (N-{3-chloro-4-[(3-fluorobenzyl)oxy]phenyl}-6-[5-({[2-(methylsulfonyl)ethy l]amino}methyl)-2-furyl]-4-quinazolinamine; GW572016). *Drug Metab Dispos* **37**:439-442.

Rao VV, Dahlheimer JL, Bardgett ME, Snyder AZ, Finch RA, Sartorelli AC and Piwnica-Worms D (1999) Choroid plexus epithelial expression of MDR1 P glycoprotein and multidrug resistance-associated protein contribute to the blood-cerebrospinal-fluid drug-permeability barrier. *Proc Natl Acad Sci U S A* **96**:3900-3905.

Reiter PD and Doron MW (1996) Vancomycin cerebrospinal fluid concentrations after intravenous administration in premature infants. *J Perinatol* **16**:331-335.

Schinkel AH, Smit JJ, van Tellingen O, Beijnen JH, Wagenaar E, van Deemter L, Mol CA, van der Valk MA, Robanus-Maandag EC, te Riele HP and et al. (1994) Disruption of the mouse mdr1a P-glycoprotein gene leads to a deficiency in the blood-brain barrier and to increased sensitivity to drugs. *Cell* **77**:491-502.

Shen DD, Artru AA and Adkison KK (2004) Principles and applicability of CSF sampling for the assessment of CNS drug delivery and pharmacodynamics. *Adv Drug Deliv Rev* **56**:1825-1857.

Sugimoto H, Hirabayashi H, Kimura Y, Furuta A, Amano N and Moriwaki T (2011) Quantitative investigation of the impact of P-glycoprotein inhibition on drug transport across blood-brain barrier in rats. *Drug Metab Dispos* **39**:8-14.

Zhou L, Schmidt K, Nelson FR, Zelesky V, Troutman MD and Feng B (2009) The effect of breast cancer resistance protein and P-glycoprotein on the brain penetration of flavopiridol, imatinib mesylate (Gleevec), prazosin, and 2-methoxy-3-(4-(2-(5-methyl-2-phenyloxazol-4-yl)ethoxy)phenyl)propanoic acid (PF-407288) in mice. *Drug Metab Dispos* **37**:946-955.

Zhuang Y, Fraga CH, Hubbard KE, Hagedorn N, Panetta JC, Waters CM and Stewart CF (2006) Topotecan central nervous system penetration is altered by a tyrosine kinase inhibitor. *Cancer Res* **66**:11305-11313.

Figure Legends

Figure 1. Effects of the 11 compounds on the transport of amprenavir in MDR1-MDCK cells at concentrations approximately corresponding to the in vivo observed maximal total plasma concentration (A) and unbound plasma concentration (B). Data points represent mean and SD from triplicate experiments.

Figure 2. Effects of the 11 compounds on the transport of prazosin in mouse Bcrp1-MDCK cells at concentrations approximately corresponding to the in vivo observed maximal total plasma concentration (A) and unbound plasma concentration (B). Data points represent mean and SD from triplicate experiments.

Figure 3. Rat plasma, brain and CSF concentration-time profiles following a discrete or cassette dose of 1-3 mg/kg. Circles, squares, and triangles represent plasma, brain and CSF concentrations, respectively. The closed and open symbols represent discrete and cassette dosing, respectively. Data points represent mean and SD from triplicate experiments.

Figure 4. Relationship between $K_{p,uu,brain}$ (A, n=9) and $K_{p,uu,CSF}$ (B, n=8) determined from discrete dosing and cassette dosing. The solid and dashed lines represent unity and 3-fold of unity, respectively. A: amprenavir, C: citalopram, D: digoxin, E: elacridar, I: imatinib, L: loperamide, P: prazosin, Q: quinidine, and V: verapamil.

Figure 5. Rat plasma, brain and CSF concentration-time profiles following a cassette dose of 1-3 mg/kg in wild-type and Mdr1a knockout rats. Circles, squares, and triangles represent plasma, brain and CSF concentrations, respectively. The closed and open symbols represent wild-type and Mdr1a knockout rats, respectively. Data points represent mean and SD from triplicate experiments.

DMD Fast Forward. Published on January 7, 2014 as DOI: 10.1124/dmd.113.055590
This article has not been copyedited and formatted. The final version may differ from this version.

Figure 6. $K_{p,uu,brain}$, $C_{u,brain}/C_{u,CSF}$, and $K_{p,uu,CSF}$ of eight compounds in wild type rats (solid bars) and Mdr1a knockout rats (open bars). The solid and dashed lines represent unity and 3-fold of unity, respectively. Data points represent mean and SD. *Statistically different with $p < 0.05$ (two-tailed t-test).

Figure 7. The relationship between the knockout/wild-type ratio of K_p in rats observed in the present study and mouse for nine compounds observed in the previous study (Liu et al., 2012). The solid and dashed lines represent unity and 3-fold of unity, respectively. A: amprenavir, C: citalopram, D: digoxin, E: elacridar, I: imatinib, L: loperamide, P: prazosin, Q: quinidine, and V: verapamil.

Table 1. Plasma and brain tissue binding (Mean ± SD).

Compound	$f_{u,plasma}$			$f_{u,brain}$		
Amprenavir	0.0992	±	0.0112	0.0687	±	0.0131
Citalopram	0.231	±	0.013	0.0306	±	0.0018
Digoxin	0.284	±	0.031	0.159	±	0.004
Elacridar	5.64E-05	±	2.70E-05	1.50E-05*	±	7.15E-06*
Imatinib	0.0169	±	0.0003	0.0441	±	0.0017
Ko143	0.0293	±	0.0051	0.00318	±	0.00030
Loperamide	0.040	±	0.002	0.00572	±	0.00064
Prazosin	0.222	±	0.008	0.107	±	0.012
Quinidine	0.274	±	0.010	0.0508	±	0.0128
Sulfasalazine	0.00232	±	0.00033	0.044	±	0.002
Verapamil	0.0582	±	0.0034	0.0220	±	0.0025

*Estimated from the mean ratio between $f_{u,plasma}$ and $f_{u,brain}$ for the other 10 compounds.

Table 2. Plasma, brain and CSF AUC and their unbound ratios (mean and SD) following discrete or cassette dosing in wild type rats from Study #1.

Compound	Discrete						Cassette					
	AUC_p (ng*h/mL)	AUC_b (ng*h/mL)	AUC_{CSF} (ng*h/mL)	$K_{p,uu,brain}$	$K_{p,uu,CSF}$	C_{ub}/C_{CSF}	AUC_p (ng*h/mL)	AUC_b (ng*h/mL)	AUC_{CSF} (ng*h/mL)	$K_{p,uu,brain}$	$K_{p,uu,CSF}$	C_{ub}/C_{CSF}
Amprenavir	853	11.3	8.86	0.0092	0.10	0.090	488	4.11	3.52	0.006	0.071	0.082
SD	127	5.7	2.08	0.0052	0.03	0.053	107	2.64	1.99	0.004	0.044	0.072
Citalopram	58.7	229	5.61	0.52	0.41	1.3	50.4	271	6.46	0.71	0.55	1.3
SD	8.3	36	1.61	0.12	0.13	0.4	10.3	109	3.14	0.33	0.29	0.8
Digoxin	1001	92.6	34.7	0.052	0.12	0.43	1472	72.6	45.3	0.028	0.11	0.26
SD	157	24.5	6.5	0.017	0.03	0.14	454	28.6	26.0	0.014	0.07	0.18
Elacridar	2.66	2.29	BLLOQ	0.23	NA	NA	2.11	2.60	BLLOQ	0.33	NA	NA
SD	0.65	0.14	BLLOQ	0.16	NA	NA	0.47	0.40	BLLOQ	0.24	NA	NA
Imatinib	183	12.6	1.35	0.18	0.37	0.49	141	13.8	1.44	0.25	0.51	0.50
SD	19	3.0	0.43	0.05	0.12	0.19	31	2.9	0.13	0.08	0.12	0.12
Ko143	BLLOQ	BLLOQ	BLLOQ	NA	NA	NA	BLLOQ	BLLOQ	BLLOQ	NA	NA	NA
SD	NA	NA	NA	NA	NA	NA	NA	NA	NA	NA	NA	NA
Loperamide	102	10.0	0.880	0.014	0.201	0.070	41.6	7.34	0.874	0.025	0.49	0.051
SD	15	2.8	0.302	0.005	0.075	0.032	6.1	1.08	0.351	0.006	0.21	0.023
Prazosin	194	43.7	6.74	0.11	0.15	0.70	146	43.7	6.37	0.15	0.20	0.74

SD	29	7.9	0.82	0.03	0.03	0.17	31	8.5	1.30	0.04	0.06	0.23
Quinidine	155	56.1	12.25	0.07	0.29	0.23	189	72.4	7.70	0.071	0.15	0.48
SD	40	11.7	4.73	0.03	0.13	0.12	38	11.1	1.83	0.026	0.05	0.18
Sulfasalazine	591	BLLOQ	BLLOQ	NA	NA	NA	373	BLLOQ	BLLOQ	NA	NA	NA
SD	123	BLLOQ	BLLOQ	NA	NA	NA	74	BLLOQ	BLLOQ	NA	NA	NA
Verapamil	75.25	45.7	1.23	0.23	0.27	0.86	61.4	45.7	2.27	0.28	0.61	0.46
SD	14.46	8.1	0.55	0.07	0.13	0.42	12.2	10.3	0.33	0.09	0.15	0.14

BLLOQ: Below the lower limit of quantitation

NA: not applicable

Table 3. Plasma, brain and CSF AUC and their unbound ratios (mean and SD) following cassette dosing in wild type and Mdr1a knockout rats from Study #2.

Compound	Wild Type Rats						Mdr1a Knockout Rats					
	AUC_p (ng*h/mL)	AUC_b (ng*h/mL)	AUC_{CSF} (ng*h/mL)	$K_{p,uu,brain}$	$K_{p,uu,CSF}$	C_{ub}/C_{CSF}	AUC_p (ng*h/mL)	AUC_b (ng*h/mL)	AUC_{CSF} (ng*h/mL)	$K_{p,uu,brain}$	$K_{p,uu,CSF}$	C_{ub}/C_{CSF}
Amprenavir	267	6.34	7.27	0.016	0.27	0.062	366	108	11.7	0.20	0.31	0.65
SD	37	4.98	2.89	0.014	0.12	0.055	81	23	4.2	0.08	0.14	0.30
Citalopram	43.1	233	8.13	0.72	0.81	0.88	50.7	880	20.3	2.3	1.7	1.3
SD	10.2	46	1.76	0.23	0.26	0.27	10.0	120	7.4	0.6	0.7	0.5
Digoxin	1580	41.5	29.3	0.015	0.065	0.23	1874	853	178	0.255	0.331	0.772
	320	30.9	6.7	0.011	0.021	0.18	381	105	54	0.067	0.127	0.255
Elacridar	0.886	1.28	BLLOQ	0.39	NA	NA	0.372	2.60	BLLOQ	1.9	NA	NA
SD	0.289	0.26	NA	0.30	NA	NA	0.174	1.13	NA	1.7	NA	NA
Imatinib	126	6.70	1.34	0.14	0.54	0.26	151	25.5	3.21	0.44	1.1	0.41
SD	42	2.24	0.48	0.07	0.26	0.13	24	3.4	0.90	0.09	0.3	0.13
Ko143	BLLOQ	BLLOQ	BLLOQ	NA	NA	NA	BLLOQ	BLLOQ	BLLOQ	NA	NA	NA
SD	NA	NA	NA	NA	NA	NA	NA	NA	NA	NA	NA	NA
Loperamide	38.6	3.59	0.204	0.013	0.12	0.11	30.0	38.6	1.02	0.18	0.79	0.23
SD	5.6	1.12	0.280	0.005	0.17	0.15	4.7	4.5	0.31	0.04	0.28	0.08
Prazosin	140	26.5	4.08	0.092	0.13	0.71	170	60.1	12.7	0.17	0.33	0.51

SD	32	5.4	1.42	0.030	0.05	0.29	22	5.9	2.9	0.03	0.09	0.14
Quinidine	148	29.9	8.85	0.038	0.22	0.17	182	1982	47.4	2.0	0.94	2.14
SD	23	5.0	2.68	0.013	0.07	0.07	32	234	12.2	0.7	0.30	0.81
Sulfasalazine	393	BLLOQ	BLLOQ	NA	NA	NA	437	BLLOQ	BLLOQ	NA	NA	NA
SD	47	NA	NA	NA	NA	NA	101	NA	NA	NA	NA	NA
Verapamil	155	74.3	5.54	0.18	0.59	0.31	182	1618	18.5	3.4	1.7	2.0
SD	21	16.8	1.92	0.05	0.22	0.13	32	325	7.6	1.0	0.8	0.9

BLLOQ: Below the lower limit of quantitation

NA: not applicable

Figure 1

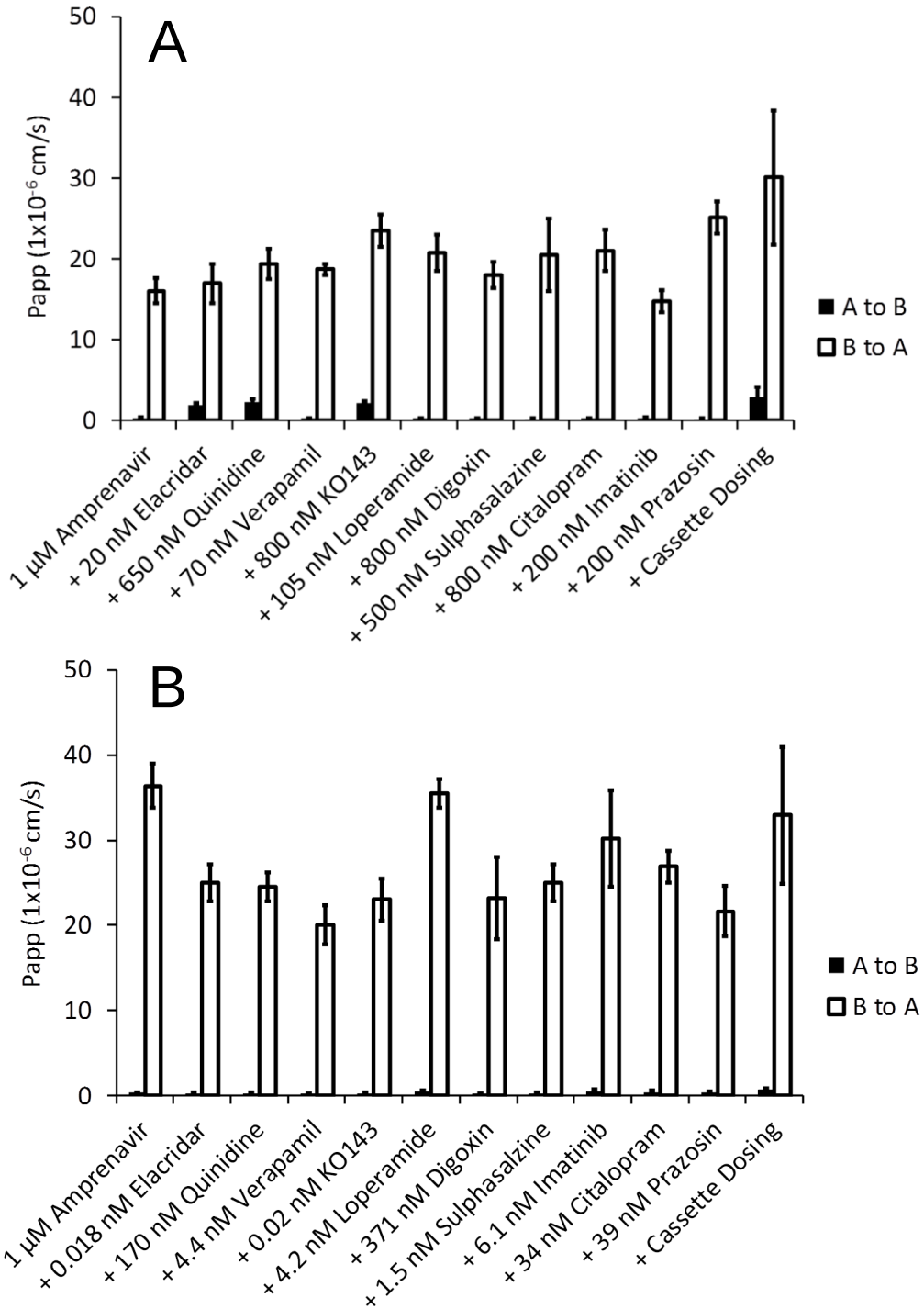

Figure 2

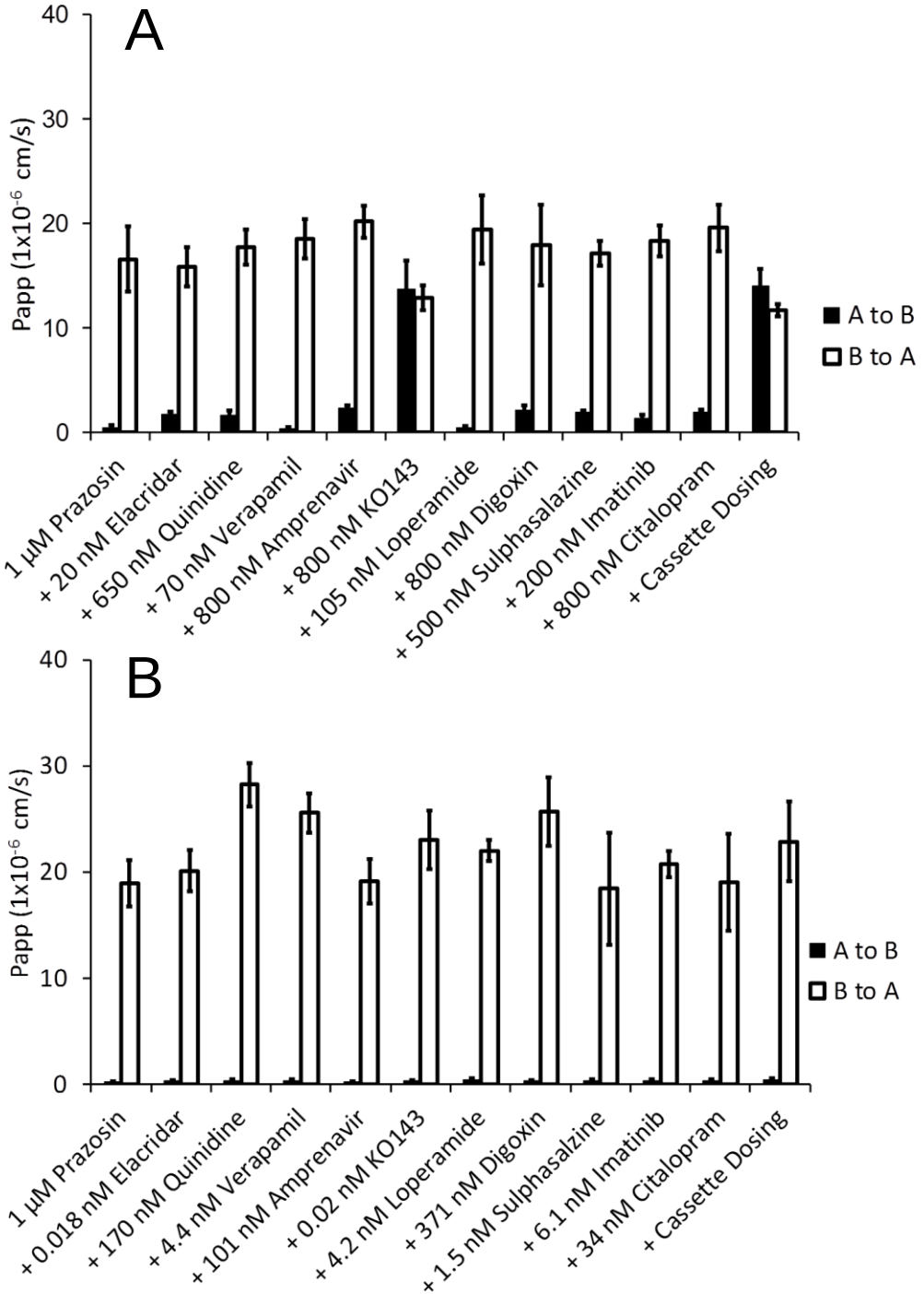

Figure 3

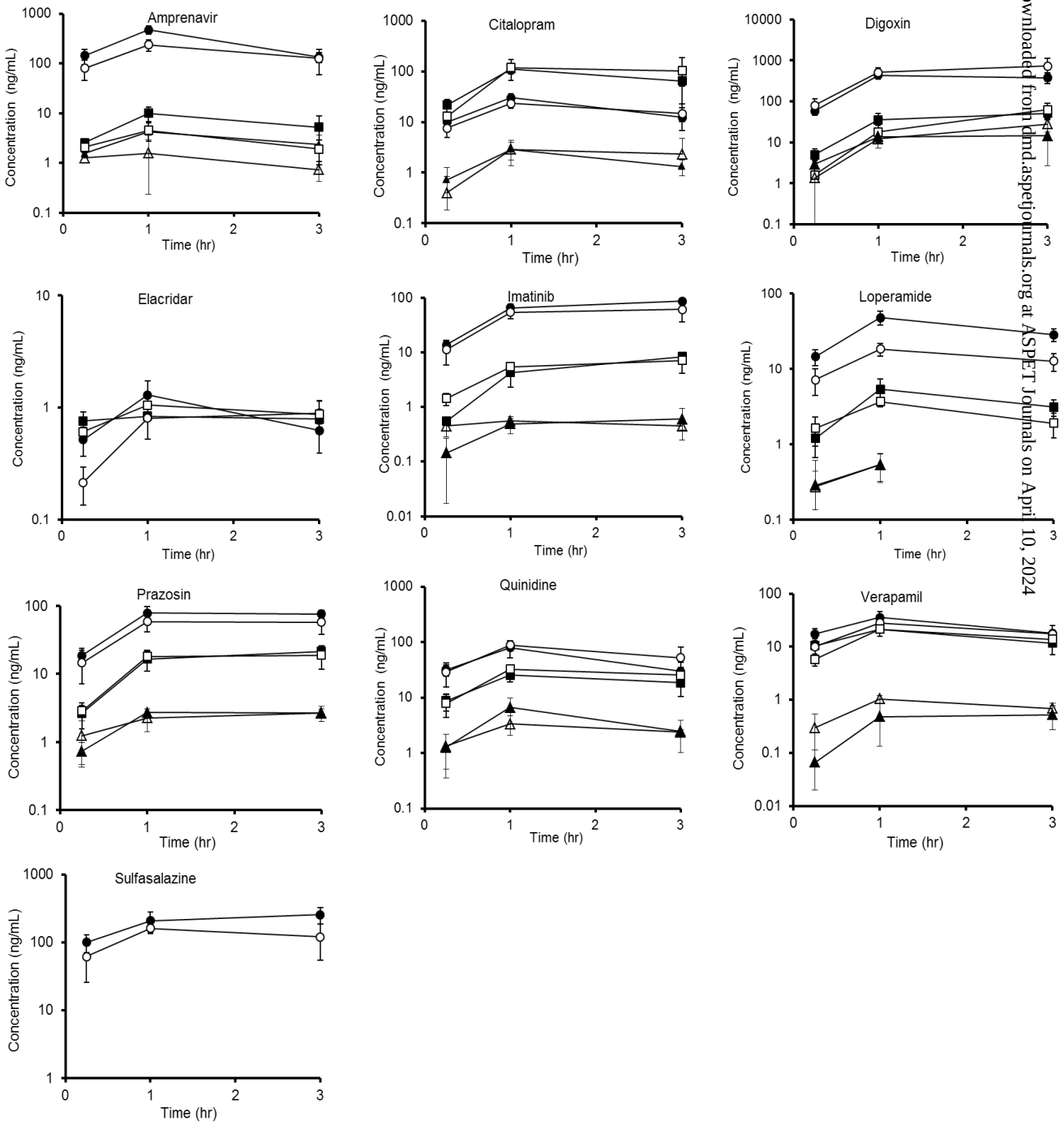

Figure 4

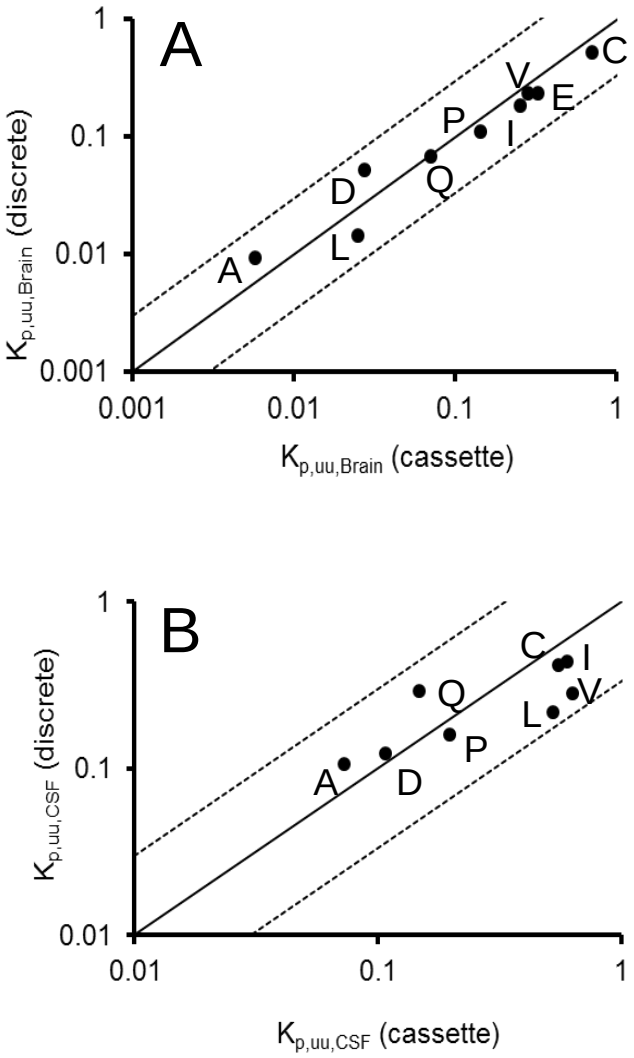

Figure 5

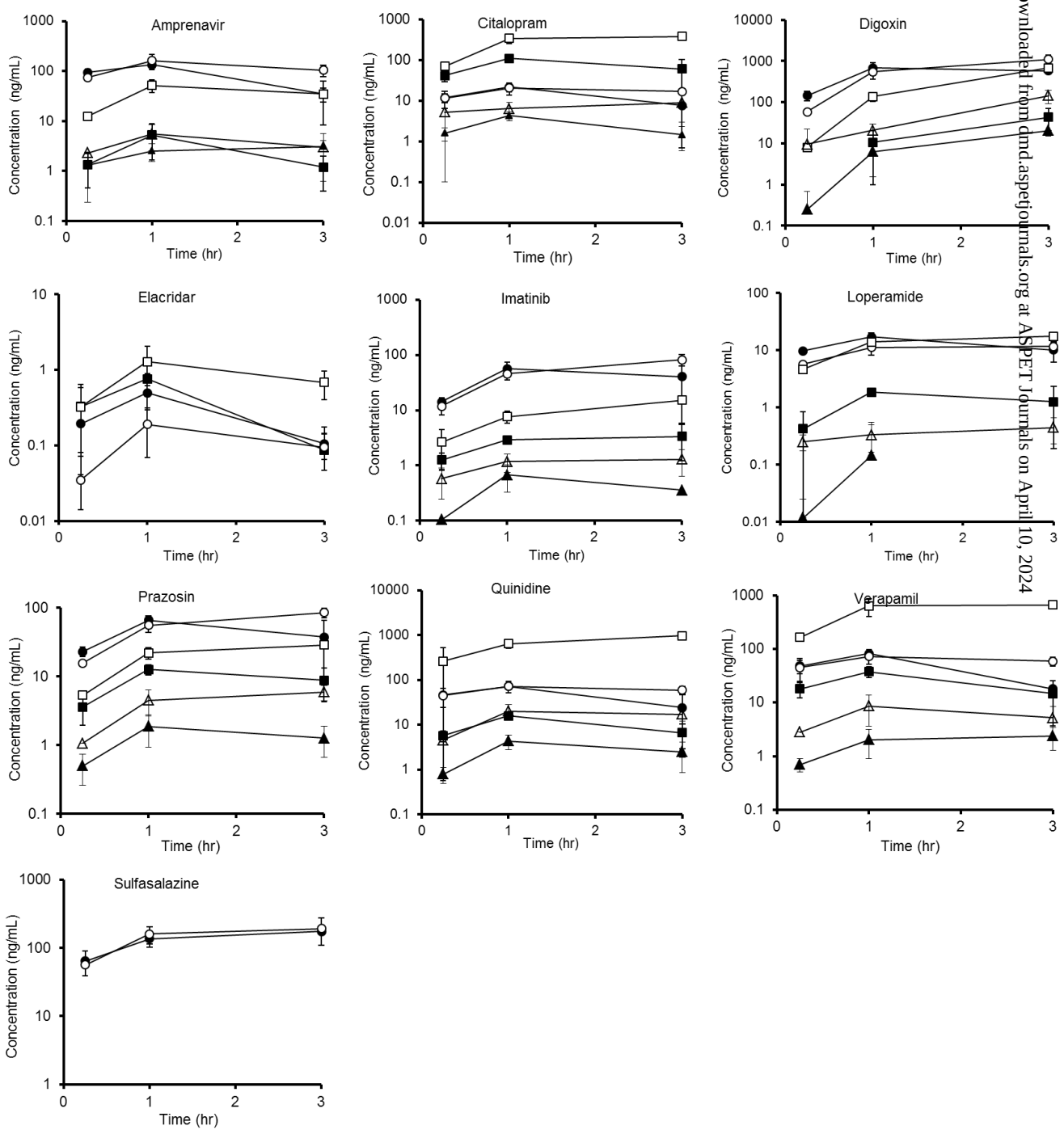

Figure 6

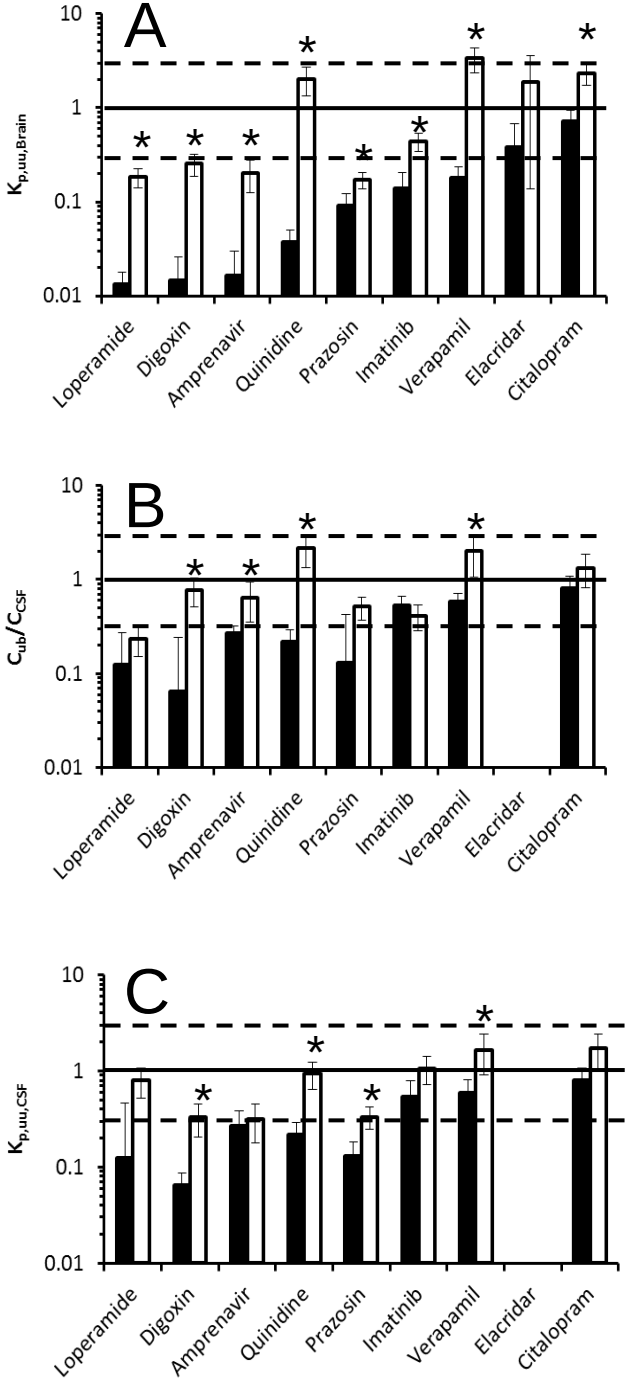

Figure 7